

Superradiance with an ensemble of superconducting flux qubits

Neill Lambert,^{1,*} Yuichiro Matsuzaki,^{2,†} Kosuke Kakuyanagi,² Natsuko Ishida,¹ Shiro Saito,² and Franco Nori^{1,3}

¹CEMS, RIKEN, Wako-shi, Saitama 351-0198, Japan

²NTT Basic Research Laboratories, NTT Corporation, 3-1 Morinosato-Wakamiya, Atsugi, Kanagawa, 243-0198, Japan

³Department of Physics, University of Michigan, Ann Arbor, Michigan 48109-1040, USA

(Received 25 July 2016; published 15 December 2016)

Superconducting flux qubits are a promising candidate for realizing quantum information processing and quantum simulations. Such devices behave like artificial atoms, with the advantage that one can easily tune the “atoms” internal properties. Here, by harnessing this flexibility, we propose a technique to minimize the inhomogeneous broadening of a large ensemble of flux qubits by tuning only the external flux. In addition, as an example of many-body physics in such an ensemble, we show how to observe superradiance, and its quadratic scaling with ensemble size, using a tailored microwave control pulse that takes advantage of the inhomogeneous broadening itself to excite only a subensemble of the qubits. Our scheme opens up an approach to using superconducting circuits to explore the properties of quantum many-body systems.

DOI: 10.1103/PhysRevB.94.224510

I. INTRODUCTION

Superconducting flux qubits (FQ) are a unique quantum technology which allow for a high degree of controllability [1–3]. With such devices high-fidelity gate operations have already been implemented [4] and quantum nondemolition measurements have been realized using Josephson bifurcation amplifiers. Moreover, since superconducting FQs behave as controllable artificial atoms, it is possible to design circuits to reach regimes typically inaccessible with real atoms [5–7].

As well as featuring high-controllability, flux qubits are attractive because it is possible to fabricate an array of FQs on the same chip [8]. Coupling such an array of *many* superconducting FQs to a common cavity (see Fig. 1 for a schematic) is important both for a range of quantum information processing tasks and for the study of quantum many-body physics [9,10], like quantum phase transitions [11–15]. In addition, an array of superconducting FQs could be used as a quantum metamaterial to control the propagation of microwaves [16–19]. Such a device also allows for the possibility of generating multiparticle entanglement between the FQs via the cavity, with the potential to employ this entanglement to improve the sensitivity of measurements [20–23].

One obstacle to such applications with an ensemble of FQs is the inhomogeneity of the FQ energies. In the context of strong coupling to a cavity, this can be overcome to some degree by using the superradiance principle [19,24,25]; if N qubits are collectively coupled with a microwave cavity, the coupling strength is enhanced by \sqrt{N} , as long as the collective coupling strength is larger than the inhomogeneous width [26–41]. Recently, by using this principle, coupling between 4300 superconducting flux qubits and a microwave resonator has been demonstrated [8]. In this experiment, spectroscopic measurements were performed by detecting the transmitted photon intensity of the resonator, and a large dispersive shift of

250 MHz has been observed. This already indicates a collective behavior involving thousands of FQs.

In this paper, we discuss how the intrinsic inhomogeneity can be reduced by a globally applied external field, an effect which we will show to be a direct consequence of the correlation between the tunneling energy and persistent current in FQs. In addition, we show how, as one of the potential applications of this device, one can observe superradiant emission from such an ensemble via the microwave cavity. Superradiance is the fascinating phenomena whereby an ensemble of atoms interacting with a common cavity or environment emits photons in a fast, collective, superradiant burst, due to correlations between atomic decay events. For this type of superradiance, the loss rate of the cavity needs to be larger than the collective coupling of the ensemble with the cavity mode, while the collective coupling strength should be much larger than the inhomogeneous width of the FQ ensemble. The observation of superradiance provides a direct signal of the collective coupling between the ensemble and the common field.

To date superradiance has been observed in various many-particle systems [42–46]. In addition, there are some experimental demonstrations of superradiance with only small ensembles of engineered quantum systems [47–51]. Typically the observation of this superradiant burst requires the careful preparation of all the atoms in their excited states, and the subsequent observation of the time-dependent photonic intensity (though steady-state driven superradiance can also

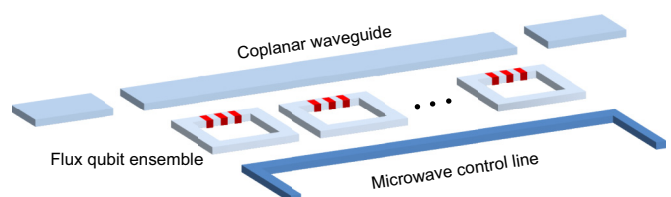


FIG. 1. Schematic of a potential flux qubit ensemble system. We estimate up to 4300 FQs can be coupled with a microwave cavity. One may characterize this system by measuring the transmission through the cavity.

*nwlambert@riken.jp

†matsuzaki.yuichiro@lab.ntt.co.jp

occur under the right conditions [52]). In the latter half of this article we show theoretically that we can prepare the ensemble of FQs with a common drive, and see not only the typical large intensity superradiance emission pulse, but also the N^2 scaling of that pulse, without local control of each qubit.

This paper is organized as follows. First, we review the recent experimental spectroscopic measurements to explain the standard properties of the system. Secondly, we introduce a scheme to suppress the inhomogeneous broadening of the FQs, which is crucial to observe superradiance and other many-body properties of such a system. Finally, we present numerical results showing how collective driving of the ensemble can selectively excite the ensemble, allowing us to directly observe the N^2 superradiant emission.

II. SPECTROSCOPIC MEASUREMENTS

The first experimental test one could make to validate a coupling between the ensemble and the cavity is to look for vacuum Rabi splitting or frequency shifts in spectroscopic measurements. In a recent experiment, spectroscopic measurements of the microwave resonator coupled with 4300 FQs [8] showed a large dispersive frequency shift, in the spectrum of the cavity, of the order of 250 MHz. Although similar signals of collective behavior have been observed in many other systems [46,53,54], for a system composed of a large FQ ensemble and a microwave resonator, this is the first strong signature of a large collective coupling [8]. There, the coupling strength between a single FQ and the resonator was estimated to be around 15 MHz, and the inhomogeneous width of the FQ frequency was between 2 and 3 GHz. Interestingly, even if there is an inhomogeneous width of a few GHz, a clear dispersive frequency shift can be observed, because the collective coupling strength ($\sqrt{N}g \simeq 1$ GHz) is comparable with the inhomogeneous width. It is worth mentioning that, in principle, one can increase this coupling strength by using a Josephson junction as a coupler [5], and so one could achieve the ultrastrong coupling regime [6,7] with this system where $\sqrt{N}g$ is both much larger than the inhomogeneous width and of the order of the flux qubit and cavity energies themselves.

III. SUPPRESSION OF THE INHOMOGENEOUS BROADENING

To observe superradiance in such an ensemble, the collective coupling strength $\sqrt{N}g$ should be larger than the variance of the frequency distribution of the FQs. Moreover, to invert the FQs using a global microwave control, the Rabi frequency of the FQs should also be larger than the inhomogeneous width, as we will describe later. However, from the direct parameters estimated in [8], it is difficult to satisfy such conditions.

To solve these problems, we propose here an approach to suppress the inhomogeneous broadening of the FQs by applying an external magnetic flux. The inhomogeneous broadening of the FQ energies comes from the nonuniform size of the Josephson junctions, which are very sensitive to small changes in fabrication conditions. We have investigated how the nonuniform Josephson junctions affect the relevant parameters of the FQs, and have found that the variation of the size of the Josephson junctions induces a *correlated*

distribution between the persistent current and tunneling energy of the FQs in the ensemble. Interestingly, due to this correlation, the inhomogeneous width of the frequencies of the FQs has a strong dependence on the applied magnetic flux, and so there exists the possibility of choosing an optimal applied magnetic flux to suppress this broadening. We predict this property could be useful to design more uniform ensembles of quantum devices, thus allowing us to observe interesting quantum many-body phenomena, such as superradiance.

To investigate how the nonuniform Josephson junctions affect the frequency distributions of a FQ, we consider the Lagrangian of a FQ with three Josephson junctions,

$$L = T - U, \quad (1)$$

$$U = \sum_{j=1}^3 \frac{\Phi_0}{2\pi} I_C^j [1 - \cos(\phi_j)], \quad (2)$$

$$T = \sum_{j=1}^3 \frac{1}{2} C_j \left(\frac{\Phi_0}{2\pi} \right)^2 \dot{\phi}_j^2, \quad (3)$$

where U is the potential energy, T is the kinetic energy, ϕ_j ($j = 1, 2, 3$) is the phase difference between the junctions, C_j is the Josephson junction capacitance, I_C^j is the critical current, Φ_0 is the external magnetic flux, and $\Phi_0 = \hbar/2e$ is the magnetic flux quantum. The phases ϕ_j ($j = 1, 2, 3$) are bounded by a condition of $\phi_1 - \phi_2 + \phi_3 = 2\pi f$ with $f = \Phi_{\text{ext}}/\Phi_0$. C_j and I_C^j have a linear dependence on the size of the junction. Here, the potential is given by $U/E_J = 2 + \alpha - \cos(\phi_p + \phi_m) - \cos(\phi_p - \phi_m) - \alpha \cos(2\pi f - 2\phi_m)$, where we set $I_C^1 = I_C^2 = I_C$, $I_C^3 = \alpha I_C$, $\phi_p = (\phi_1 + \phi_2)/2$, and $\phi_m = (\phi_1 - \phi_2)/2$. If we set $\phi_p = 0$ and $f = 0.5$, we have $\frac{dU}{df} = 2E_J \sin \phi_m (1 - 2\alpha \cos \phi_m)$, and so the potential shows minima for $\pm \phi_m^*$, where $\cos \phi_m^* = 1/(2\alpha)$. We plot this potential in Fig. 2. By solving the Lagrangian, we can calculate the tunneling energy and persistent current [55]. We set $E_J/E_c = 75$ for our simulations, where $E_J^{(j)} = \frac{\Phi_0}{2\pi} I_C^j$ ($E_c = e^2/2C_j$) is the characteristic scale of the Josephson (electric) energy.

Usually, the size of one of the three junctions is designed to be α times smaller than the other two junctions [55]. However, with current technology it is difficult to fabricate homogenous junctions, and this results in a random distribution of the tunneling energy and the persistent current. We assume a Gaussian distribution for the normalized areas of the smaller

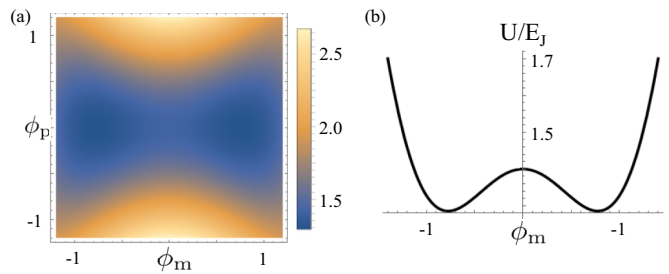


FIG. 2. Potential of the flux qubit. We set $\alpha = 0.7$ and $f = 0.5$. There are two minima separated by an energy barrier. (a) The density plot of the potential. (b) A plot of the potential against ϕ_m for $\phi_p = 0$.

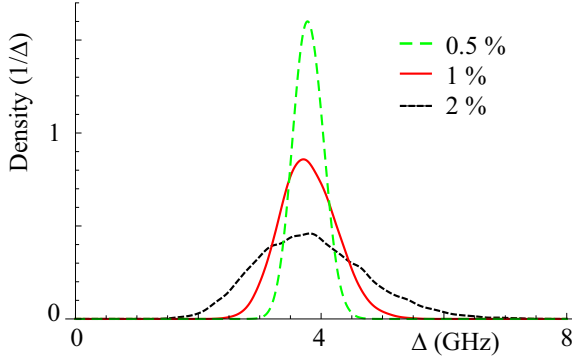


FIG. 3. Probability density of the tunneling energies of the flux qubits when the size of the Josephson junctions are nonuniform. There are three Josephson junctions in the superconducting circuit, and the size of one Josephson junction is designed to be smaller than the size of the other two junctions. We assume a Gaussian distribution for normalized areas of the smaller junction (two larger junctions) where we have the mean value of $\bar{\alpha} = 0.7$ ($\bar{\beta}_k = 1$ for $k = 1, 2$) and the standard deviation of σ_S ($\sigma_L^{(k)}$ for $k = 1, 2$). We set the parameters as $\sigma_S/\bar{\alpha} = \sigma_L^{(1)}/\bar{\beta} = \sigma_L^{(2)}/\bar{\beta} = 0.5\%, 1\%, 2\%$ respectively, and obtain the values of Δ_j ($j = 1, 2, \dots, N$) from numerical simulations. To plot the density of the tunneling energy, we use a kernel density estimator $\sum_{j=1}^N K(\frac{\Delta - \Delta_j}{h})$, where we set $K(x) = \frac{1}{\sqrt{2\pi}} \exp(-\frac{1}{2}x^2)$, $N = 10000$, and $h = 0.1$ GHz.

junction (two larger junctions), where we have the mean value of $\bar{\alpha}$ ($\bar{\beta}_k$ for $k = 1, 2$) and the standard deviation of σ_S ($\sigma_L^{(k)}$ for $k = 1, 2$).

First, in Fig. 3 we plot the distribution of the tunneling energies of the FQ. This confirms that the nonuniform Josephson junctions affect the random distribution of the tunneling energy. As expected, as we increase the width of the distribution of the Josephson junction size, the width of the tunneling energy distribution also increases.

Secondly, we plot the distribution of the persistent current and tunneling energy given by the nonuniform Josephson junctions in Fig. 4. We randomly generate the values of the

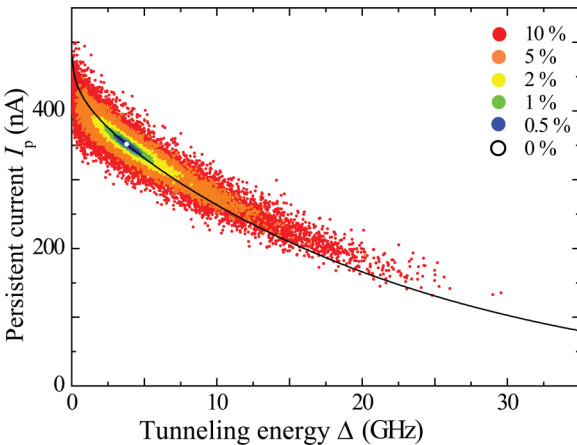


FIG. 4. Persistent currents and tunneling energies of FQs with random-size Josephson junctions. We set the same parameters as in Fig. 3. There is a clear correlation between the tunneling energy Δ and persistent current I_p .

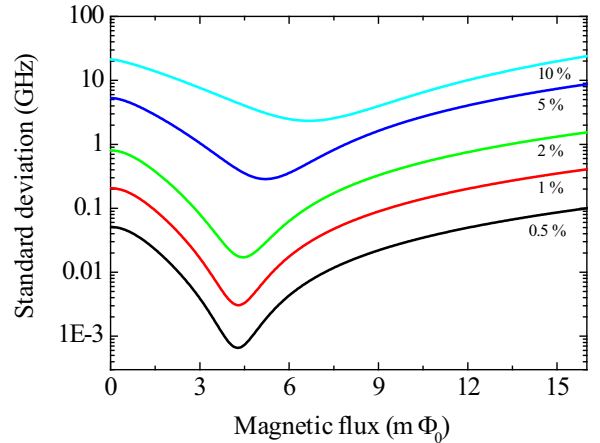


FIG. 5. Standard deviation of the distribution of the flux qubit frequencies versus the applied magnetic flux. We set the same parameters as in Fig. 3. The standard deviation strongly depends on the applied magnetic flux.

Josephson junction size, and calculate the resulting tunneling energy and persistent current. This result clearly show a correlation between the tunneling energy and persistent current where a FQ with a higher tunneling energy tends to have a lower persistent current. We can qualitatively explain this correlation as follows. As we increase the value of α , the potential gradient $\frac{dU}{df} \simeq 2\pi E_J [1 - \frac{1}{(2\alpha)^2}]^{1/2}$ becomes larger for $\phi_p \simeq 0$, $\phi_m \simeq \phi_m^*$, and $f \simeq 0.5$. A larger potential gradient makes the energy of the FQ more sensitive to the change in the applied magnetic flux, which corresponds to a higher persistent current. On the other hand, as we increase the value of α , the tunneling barrier $E_t = U(\phi_m = 0) - U(\phi_m = \phi_m^*) = E_J(-2 + 2\alpha + \frac{1}{2\alpha})$ becomes larger for $\phi_p \simeq 0$, $\phi_m \simeq \phi_m^*$, $\alpha \simeq 0.7$, and $f \simeq 0.5$. The larger tunneling barrier suppresses the tunneling energy of the FQ. Therefore, if the persistent current becomes larger, the tunneling energy is expected to be smaller, which is consistent with our numerical simulations. Moreover, it is worth mentioning that a similar model was used to reproduce the experimental results in [8] where spectroscopy of a microwave resonator coupled to 4300 FQs was performed and good agreement between numerical and experimental results was observed [8]. In that experiment, the standard deviation of the Josephson junction size is around a few percent, which corresponds to the yellow region in Fig. 4.

Thirdly, in Fig. 5 we plot the standard deviation of the FQ frequency distribution against an applied magnetic field. Interestingly, these results show that the standard deviation of the frequency distribution strongly depends on the applied magnetic flux; there exists an optimal point where the standard deviation of the flux qubit frequency becomes minimum. The width of the distribution becomes one or two orders of magnitude smaller at the optimal point than elsewhere. This can be understood as a consequence of the correlation between the tunneling energy and the persistent current, as shown in Fig. 6.

To illustrate this idea, let us consider a pair of flux qubits with different junction sizes. The FQ energy is given by $\omega_j = \sqrt{|\epsilon_j|^2 + |\Delta_j^{(0)}|^2}$, for $\epsilon_j = 2I_j(\Phi_{\text{ext}} - \frac{1}{2}\Phi_0)$ ($j = 1, 2$), and we can assume $\Delta_1^{(0)} > \Delta_2^{(0)}$ without loss of generality.

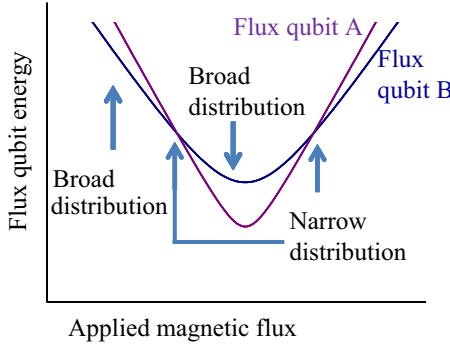


FIG. 6. Energies of two flux qubits (A and B), with different size junctions, as a function of an applied magnetic field. The flux qubit energy is represented by $\omega_j = \sqrt{|\epsilon_j|^2 + |\Delta_j^{(t)}|^2}$ for $\epsilon_j = 2I_j(\Phi_{\text{ext}} - \frac{1}{2}\Phi_0)$, where Φ_{ext} denotes the applied magnetic flux. Flux qubit A has a smaller (larger) tunneling energy (persistent current) than B. In this case, we can make the frequency of the qubits the same by applying an appropriate amount of the applied magnetic flux.

Interestingly, when $I_1 < I_2$, which is the expected statistical relationship given $\Delta_1 > \Delta_2$, we can show that there exists an optimal flux such that $\omega_1 = \omega_2$ is satisfied. So we can balance the two flux qubit energies just by applying a global magnetic flux. This means that, even if we have several qubits with different-size Josephson junctions, if there is a correlation such that a smaller persistent current I_j tends to increase the tunneling energy $\Delta_j^{(t)}$, we can make the frequency of these qubits similar by tuning an external magnetic flux, as shown in Fig. 4.

IV. SUPERRADIANCE

To illustrate how such an ensemble with a reduced inhomogeneous width can lead to observable collective effects, we numerically simulate [56,57] a small ensemble with an explicit inhomogeneity. We also show how this residual inhomogeneity can be used as a tool to aid initial-state preparation. We explicitly model $N = 10$ FQs, with inhomogeneous normally distributed energies ω_j with mean value $\bar{\omega}_j$ and variance $\delta\omega_j$. These qubits are coupled to a single common microwave cavity of frequency ω_c with a common homogenous coupling strength g . The general Hamiltonian for such a system reads

$$H = \sum_{j=1}^N \frac{\omega_j}{2} \sigma_z^{(j)} + \omega_c a^\dagger a + g(J_- a^\dagger + J_+ a), \quad (4)$$

where $J_+ = \sum_j \sigma_+^{(j)}$, $J_- = \sum_j \sigma_-^{(j)}$, and we have set $\hbar = 1$ for simplicity. In general, we assume that the cavity decay, with rate κ , is given by a Lindblad superoperator $\kappa \mathcal{D}[a]$, where $D[a] = 2a a^\dagger - a^\dagger a p - p a^\dagger a$.

To begin with, we eliminate the cavity [58,59], assuming the bad-cavity limit: $\kappa \gg \delta\omega_j, g^2 N / \kappa$ (superradiance is also possible in the dispersive good-cavity limit; see the Appendix). In this bad-cavity case the equation of motion is reduced to the following form:

$$H_{\text{AE}} = \sum_{j=1}^N \frac{(\omega_j - \bar{\omega}_j)}{2} \sigma_z^{(j)} + (\omega_c - \bar{\omega}_j) \frac{g^2}{\Gamma^2} J_+ J_-, \quad (5)$$

where $\Gamma = \kappa + i(\omega_c - \bar{\omega}_j)$. There also arises a new loss term, $S[\rho] = \kappa \frac{g^2}{\Gamma^2} \mathcal{D}[J_-] \rho$. It is this term that induces the superradiance phenomena, and we expect to observe such superradiance when $\delta\omega_j \ll g^2 N / \kappa$.

Even though the cavity is eliminated, one can estimate the intensity of the radiation emitted from the qubits from the squared atomic polarization [58],

$$I(t) = \frac{2g^2}{\kappa} \omega_c \langle J_+(t) J_-(t) \rangle. \quad (6)$$

Typically the intensity grows with time, reaches a maximum at the peak superradiance time $\tau_{\text{sr}} = \kappa/g^2 N$ and then decays. The successful observation of this pulse requires that the coherence time of the qubits is longer than the expected peak superradiance time. Assuming dephasing is dominated by the inhomogeneity of the energies of the FQs, we can assess the visibility of superradiance via the parameter $\tilde{\alpha} = T_2^*/\tau_{\text{sr}} = Ng^2/\kappa\delta\omega_j$, where T_2^* is the inhomogeneous dephasing time.

In addition to the qubits being inhomogeneous, the direct control of individual qubits is challenging. However, we can consider collective ways in which to prepare spin-polarized states, which we can be used to observe superradiance. In particular, by strongly driving the cavity, or using another common control line, as per Fig. 1, we can induce a time-dependent collective control term, such that the dynamics of the qubits can be written as

$$H_{\text{drive}} = \sum_{j=1}^N \frac{\omega_j}{2} \sigma_z^{(j)} + \lambda(t) \cos(\omega_d t) \sum_j \sigma_x^{(j)}, \quad (7)$$

$$H'_{\text{drive}} \approx \sum_{j=1}^N \frac{\Delta'_j}{2} \sigma_z^{(j)} + \frac{\lambda(t)}{2} \sum_j \sigma_x^{(j)}, \quad (8)$$

where in the second equation we moved to a frame rotating at the drive frequency, such that $\Delta'_j = \omega_j - \omega_d$, and made a rotating-wave approximation. Later we will choose the drive to be resonant with the average value of the qubit energies $\omega_d = \bar{\omega}_j$. If we consider just a single qubit, initially in its ground state, we know that if we apply a drive of strength λ for a period $T_\pi = \pi/\lambda$ we will find that the spin has a probability of being in its excited state:

$$P_{\text{exc}} = \frac{\lambda^2}{\Delta_j^2 + \lambda^2}. \quad (9)$$

Extending this notion to N spins we expect that we will have an effective excited number of spins $M_{\text{eff}} = \sum_j \frac{\lambda^2}{\Delta_j^2 + \lambda^2}$. Thus simply changing the magnitude of λ enables us to effectively control the number of spins contributing to the superradiance emission (up to the limit of validity of the rotating wave approximation). In addition, one can also control the shape of the envelope of the drive, $\lambda(t)$. While P_{exc} and M_{eff} only apply for a step-function envelope, they provide a useful estimate. In practice we found that a Gaussian function for $\lambda(t)$ worked best in preparing the desired initial state, and thus only show that example here. In principle one can also use more sophisticated techniques from quantum control theory to prepare the desired state [60–62].

Importantly, when we need to excite most of the qubit ensemble, the drive, or Rabi frequency, λ should be as large or

larger than the inhomogeneous width. Although it is possible to achieve a Rabi frequency of a few GHz [63] for a single FQ, it is not straightforward to realize such a strong driving condition for a large ensemble. For this reason, it is crucial to decrease the width of the inhomogeneous broadening of the FQs by, for example, applying a magnetic flux, as described earlier. This will allow us to both excite the ensemble with moderate values of λ , and observe superradiance with accessible values of g .

To obtain numerical results we solve the master equation for all N qubits explicitly by generating a random ensemble of energies, preparing the qubit ensemble in the common ground state (without interaction with the cavity) $\psi(0) = |0\rangle_1 \otimes |0\rangle_2 \otimes \dots \otimes |0\rangle_N$, and then “switch on” the driving term $H'_{\text{drive}}(t)$ for a period τ such that $\int_0^\tau \lambda(t) \approx \pi$. We assume that during this driving period the cavity and qubit ensemble are far off-resonance. In other words, the ensemble evolves under the free evolution of the ensemble Hamiltonian and the drive, given by $H'_{\text{drive}}(t)$ in Eq. (8), without influence from the cavity. In principle, this implies we also require that the period τ is shorter than the relaxation time of the qubits.

After this evolution, we record the effective number of excited qubits $M = \langle \sum_j \sigma_z^{(j)} \rangle$, switch off the drive, and allow the system to evolve under both H_{AE} and the superradiant loss term $S[\rho] = \kappa \frac{g^2}{\Gamma^2} \mathcal{D}[J_-] \rho$, as determined by the master equation

$$\dot{\rho} = -\frac{i}{\hbar} [H_{\text{AE}}, \rho] + S[\rho] \quad (10)$$

for a time interval much longer than τ_{sr} (recalling $\tau_{\text{sr}} = \kappa/g^2 M$, where M are the number of qubits excited by the drive). For this period of evolution we record the cavity emission intensity by calculating $I(t)$, and from this measurement record the maximum (over time) acquired value $\text{Max}[\langle J_+ J_- \rangle]$. Under perfect superradiance $\text{Max}[\langle J_+ J_- \rangle]$ should scale as M^2 .

We repeat this procedure as a function of the driving strength λ , and plot the recorded maximum intensity $\text{Max}[\langle J_+ J_- \rangle]$ as a function of M , the effective number of qubits initially excited by the drive. Figure 7 shows this for a Gaussian drive shape $\lambda(t) = \lambda_{\text{max}} \exp[-(\frac{t-b}{\sigma})^2]$ with $\sigma = \sqrt{\pi}/\lambda_{\text{max}}$ and $b = 4\sigma\sqrt{2 \ln 2}$. This is compared to the test case where the actual number of initially excited qubits is enforced “by hand,” which we refer to as the “discrete M ” case. We now see that the drive prepares a subset of the qubits in their excited states, thus altering the resultant photonic emission intensity. This allows us to directly observe the quadratic scaling of that intensity as a function of the number of qubits contributing to the collective decay. For the parameters chosen here, we see the onset of superradiance when M becomes greater than about four (see caption of Fig. 7).

In practice, as the number of FQs increases, one can still see superradiance for much larger values of the inhomogeneity, or smaller couplings, than we show here. For example, from the simulations described above, we can extrapolate the behavior of a device composed of 4300 FQs coupled with the microwave cavity. Due to the form of the loss term $S[\rho] = \frac{g^2}{\kappa} \mathcal{D}[J_-] \rho$, for $\omega_c = \bar{\omega}_j$, we should have a similar behavior for the emitted intensity from the cavity, as long as the value of Mg^2/κ is the same. Thus, if we fabricate a device with $g = 5$ MHz,

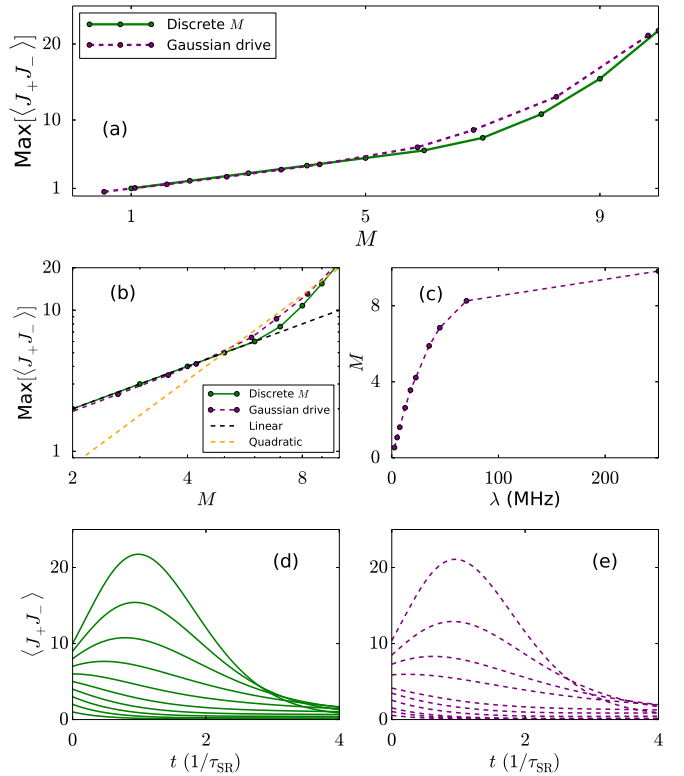


FIG. 7. (a) Maximum (over time) emitted intensity versus number of initially excited qubits M . For discrete M (green solid curve) we artificially prepare a subset M of the total ensemble of N qubits in their excited states. In the other case (purple dashed line), at $t = 0$ we prepare all qubits in their ground state and then evolve with the Hamiltonian $H_{\text{drive}}(t)$ switched on, with a Gaussian function envelope $\lambda(t)$, as described in the main text. We then switch off the driving and allow the system to evolve under the influence of Eq. (10), and record the maximum emitted intensity over a time period exceeding the expected superradiant pulse duration. We do this for a range of λ_{max} , which induce an effective number M of qubits to become excited. For the other parameters we set $\bar{\omega}_j = \omega_c$, $\delta\omega_j = 25$ MHz, $g = 50$ MHz, $\kappa = 400$ MHz, and $N = 10$, so as to give a value for $\tilde{\alpha} > 1$ as M becomes greater than 4. Panel (b) shows the logarithmic intensity, which changes from linear to quadratic behavior as M passes this $M = 4$ threshold (the gray dotted line is an artificial linear comparison curve, while the orange dotted line is an artificial quadratic comparison curve, to show this change clearly). Panel (c) shows the explicit λ_{max} values used in the Gaussian drive, and the associated number of excited spins M in the ensemble after the drive has been applied. Panel (d) shows the explicit time-dependent curves of intensity for different values of M , increasing from the bottom up, starting with $M = 1$ to 10, from which the green dotted-dashed line in figure (a) is extracted. The change from normal to superradiant emission around $M = 4$ is clear. Similarly, panel (e) shows the same curves for the driven state preparation example. Note that all curves are averaged over a large set of randomly generated ensemble energies.

$\delta\omega_j = 25$ MHz, $\kappa = 1.72$ GHz, and $N = 4300$, and excite the full ensemble, so that $M = N$, the value of Mg^2/κ coincides with that used in our numerical simulation with 10 excited qubits; and so we should be able to observe the quadratic scaling of the intensity for this case as well. This means that

one can see superradiance from 4300 FQs even for coupling strengths as small as 5 MHz.

V. CONCLUSIONS

We have shown that, even though large ensembles of FQs suffer from intrinsic fabrication-induced inhomogeneities, this can be minimized by tuning the ensemble FQs properties with an external flux. This opens up the possibility of observing collective many-body effects, a simple example of which we give in terms of superradiant emission into a microwave cavity. We expect that such large ensembles will enable the investigation of a range of interesting physics in the future, including criticality [11–15], macroscopic coherence [64,65], and spin squeezing [20–23].

ACKNOWLEDGMENTS

This work was supported by JSPS KAKENHI Grant No. 15K17732, JSPS KAKENHI Grant No. 25220601, the Commissioned Research No. 158 of NICT, and MEXT KAKENHI Grant No. 15H05870. F.N. and N.L. acknowledge support from the Sir John Templeton Foundation. F.N. acknowledges support from the RIKEN iTHES Project, the MURI Center for Dynamic Magneto-Optics via the AFOSR Award No. FA9550-14-1-0040, the IMPACT program of JST, CREST, and a Grant-in-Aid for Scientific Research (A). N.L. and Y.M. contributed equally to this work.

APPENDIX: DISPERSIVE SUPERRADIANCE MODEL

One can also obtain collective superradiant decay due to interaction with a common cavity by moving to a dispersive coupling regime [22], where the cavity and qubits are off-resonance, without necessarily demanding that the cavity losses be large. Starting again with Eq. (4) one can apply the transformation $e^R H_{DE} e^{-R}$, where $R = \frac{g}{\chi}(J_- a^\dagger - J_+ a)$, $\chi = \omega_c - \bar{\omega}_j$, and keeping terms to order $(g/\chi)^2$ find that

$$H_{\text{disp}} = \sum_{j=1}^N \left(\frac{1}{2} \omega_j + \beta a^\dagger a \right) \sigma_z^{(j)} + \frac{\beta}{2} J_+ J_-, \quad (\text{A1})$$

where $\beta = 2g^2/\chi$ and again a new loss term arises,

$$\mathcal{S}_{\text{disp}} = \kappa \frac{g^2}{\chi^2} \mathcal{D}[J_-] \rho. \quad (\text{A2})$$

One expects in this case that superradiance will occur when $g^2 N \kappa / \chi^2 \gg \delta \omega_j$, giving an equivalent parameter to assess the visibility $\alpha_D = g^2 N \kappa / (\chi^2 \delta \omega_j)$. However, this regime is valid for $(g/\chi)^2 \ll 1$, which implies $N \kappa / \delta \omega_j \gg (g/\chi)^2$. As with the adiabatic elimination case, the spin squeezing term $J_+ J_-$ does not affect the superradiance dynamics significantly.

-
- [1] J. Q. You and F. Nori, Atomic physics and quantum optics using superconducting circuits, *Nature (London)* **474**, 589 (2011).
- [2] J. Clarke and F. K. Wilhelm, Superconducting quantum bits, *Nature (London)* **453**, 1031 (2008).
- [3] I. Buluta, S. Ashhab, and F. Nori, Natural and artificial atoms for quantum computation, *Rep. Prog. Phys.* **74**, 104401 (2011).
- [4] J. Bylander, S. Gustavsson, F. Yan, F. Yoshihara, K. Harrabi, G. Fitch, D. G. Cory, Y. Nakamura, J. S. Tsai, and W. D. Oliver, Noise spectroscopy through dynamical decoupling with a superconducting flux qubit, *Nat. Phys.* **7**, 565 (2011).
- [5] F. Yoshihara, T. Fuse, S. Ashhab, K. Kakuyanagi, S. Saito, and K. Semba, Superconducting qubit-oscillator circuit beyond the ultrastrong-coupling regime, *Nat. Phys.* (2016), doi:10.1038/nphys3906.
- [6] Z. Chen, Y. Wang, T. Li, L. Tian, Y. Qiu, K. Inomata, F. Yoshihara, S. Han, F. Nori, J. S. Tsai, and J. Q. You, Multi-photon sideband transitions in an ultrastrongly-coupled circuit quantum electrodynamics system, *arXiv:1602.01584*.
- [7] P. Forn-Díaz, J. J. García-Ripoll, B. Peropadre, M. A. Yurtalan, J.-L. Orgiazzi, R. Belyansky, C. M. Wilson, and A. Lupascu, Ultrastrong coupling of a single artificial atom to an electromagnetic continuum, *Nat. Phys.* (2016), doi:10.1038/nphys3905.
- [8] K. Kakuyanagi, Y. Matsuzaki, C. Deprez, H. Toida, K. Semba, H. Yamaguchi, W. J. Munro, and S. Saito, Observation of Collective Coupling Between an Engineered Ensemble of Macroscopic Artificial Atoms and a Superconducting Resonator, *Phys. Rev. Lett.* **117**, 210503 (2016).
- [9] I. Buluta and F. Nori, Quantum simulators, *Science* **326**, 108 (2009).
- [10] I. M. Georgescu, S. Ashhab, and F. Nori, Quantum simulation, *Rev. Mod. Phys.* **86**, 153 (2014).
- [11] K. Hepp and E. H. Lieb, On the superradiant phase transition for molecules in a quantized radiation field: The Dicke Maser model, *Ann. Phys. (N.Y.)* **76**, 360 (1973).
- [12] Y. K. Wang and F. T. Hioe, Phase transition in the Dicke model of superradiance, *Phys. Rev. A* **7**, 831 (1973).
- [13] C. Emary and T. Brandes, Chaos and the quantum phase transition in the Dicke model, *Phys. Rev. E* **67**, 066203 (2003).
- [14] N. Lambert, Y.-n. Chen, R. Johansson, and F. Nori, Quantum chaos and critical behavior on a chip, *Phys. Rev. B* **80**, 165308 (2009).
- [15] N. Lambert, C. Emary, and T. Brandes, Entanglement and the Phase Transition in Single-Mode Superradiance, *Phys. Rev. Lett.* **92**, 073602 (2004).
- [16] A. L. Rakhmanov, A. M. Zagoskin, S. Savel'ev, and F. Nori, Quantum metamaterials: Electromagnetic waves in a Josephson qubit line, *Phys. Rev. B* **77**, 144507 (2008).
- [17] C. M. Soukoulis and M. Wegener, Past achievements and future challenges in the development of three-dimensional photonic metamaterials, *Nat. Photon.* **5**, 523 (2011).
- [18] N. I. Zheludev and Y. S. Kivshar, From metamaterials to metadevices, *Nat. Mater.* **11**, 917 (2012).
- [19] P. Macha, G. Oelsner, J. M. Reiner, M. Marthaler, S. André, G. Schön, U. Hübner, H. G. Meyer, E. Illich, and A. V. Ustinov, Implementation of a quantum metamaterial using superconducting qubits, *Nat. Commun.* **5**, 5146 (2014).

- [20] M. Kitagawa and M. Ueda, Squeezed spin states, *Phys. Rev. A* **47**, 5138 (1993).
- [21] J. Ma, X. Wang, C. P. Sun, and F. Nori, Quantum spin squeezing, *Phys. Rep.* **509**, 89 (2011).
- [22] S. D. Bennett, N. Y. Yao, J. Otterbach, P. Zoller, P. Rabl, and M. D. Lukin, Phonon-induced Spin-spin Interactions in Diamond Nanostructures: Application to Spin Squeezing, *Phys. Rev. Lett.* **110**, 156402 (2013).
- [23] T. Tanaka, P. Knott, Y. Matsuzaki, S. Dooley, H. Yamaguchi, W. J. Munro, and S. Saito, Proposed Robust Entanglement-based Magnetic Field Sensor Beyond the Standard Quantum Limit, *Phys. Rev. Lett.* **115**, 170801 (2015).
- [24] A. İmamoğlu, Cavity QED Based on Collective Magnetic Dipole Coupling: Spin Ensembles as Hybrid Two-level Systems, *Phys. Rev. Lett.* **102**, 083602 (2009).
- [25] J. H. Wesenberg, A. Ardavan, G. A. D Briggs, J. J. L. Morton, R. J. Schoelkopf, D. I. Schuster, and K. Mølmer, Quantum Computing with an Electron Spin Ensemble, *Phys. Rev. Lett.* **103**, 070502 (2009).
- [26] Z.-L. Xiang, S. Ashhab, J. Q. You, and F. Nori, Hybrid quantum circuits: Superconducting circuits interacting with other quantum systems, *Rev. Mod. Phys.* **85**, 623 (2013).
- [27] D. I. Schuster, A. P. Sears, E. Ginossar, L. DiCarlo, L. Frunzio, J. J. L. Morton, H. Wu, G. A. D. Briggs, B. B. Buckley, D. D. Awschalom, and R. J. Schoelkopf, High-cooperativity Coupling of Electron-spin Ensembles to Superconducting Cavities, *Phys. Rev. Lett.* **105**, 140501 (2010).
- [28] H. Wu, R. E. George, J. H. Wesenberg, K. Mølmer, D. I. Schuster, R. J. Schoelkopf, K. M. Itoh, A. Ardavan, J. J. L. Morton, and G. A. D. Briggs, Storage of Multiple Coherent Microwave Excitations in an Electron Spin Ensemble, *Phys. Rev. Lett.* **105**, 140503 (2010).
- [29] Y. Kubo, F. R. Ong, P. Bertet, D. Vion, V. Jacques, D. Zheng, A. Dréau, J. F. Roch, A. Auffeves, F. Jelezko, J. Wrachtrup, M. F. Barthe, P. Bergonzo, and D. Esteve, Strong Coupling of a Spin Ensemble to a Superconducting Resonator, *Phys. Rev. Lett.* **105**, 140502 (2010).
- [30] R. Amsüss, C. H. Koller, T. Nöbauer, S. Putz, S. Rotter, K. Sandner, S. Schneider, M. Schramböck, G. Steinhauser, H. Ritsch, J. Schmiedmayer, and J. Majer, Cavity QED with Magnetically Coupled Collective Spin States, *Phys. Rev. Lett.* **107**, 060502 (2011).
- [31] Y. Kubo, C. Grezes, A. Dewes, T. Umeda, J. Isoya, H. Sumiya, N. Morishita, H. Abe, S. Onoda, T. Ohshima, V. Jacques, A. Dreau, J. F. Roch, I. Diniz, A. Auffeves, D. Vion, D. Esteve, and P. Bertet, Hybrid Quantum Circuit with a Superconducting Qubit Coupled to a Spin Ensemble, *Phys. Rev. Lett.* **107**, 220501 (2011).
- [32] X. Zhu, S. Saito, A. Kemp, K. Kakuyanagi, S. Karimoto, H. Nakano, W. J. Munro, Y. Tokura, M. S. Everitt, K. Nemoto, M. Kasu, N. Mizuochi, and K. Semba, Coherent coupling of a superconducting flux qubit to an electron spin ensemble in diamond, *Nature (London)* **478**, 221 (2011).
- [33] Y. Kubo, I. Diniz, A. Dewes, V. Jacques, A. Dréau, J. F. Roch, A. Auffèves, D. Vion, D. Esteve, and P. Bertet, Storage and retrieval of a microwave field in a spin ensemble, *Phys. Rev. A* **85**, 012333 (2012).
- [34] Y. Kubo, I. Diniz, C. Grezes, T. Umeda, J. Isoya, H. Sumiya, T. Yamamoto, H. Abe, S. Onoda, T. Ohshima, V. Jacques, A. Dreau, J. F. Roch, A. Auffèves, D. Vion, D. Esteve, and P. Bertet, Electron spin resonance detected by a superconducting qubit, *Phys. Rev. B* **86**, 064514 (2012).
- [35] D. Marcos, M. Wubs, J. M. Taylor, R. Aguado, M. D. Lukin, and A. S. Sørensen, Coupling Nitrogen-vacancy Centers in Diamond to Superconducting Flux Qubits, *Phys. Rev. Lett.* **105**, 210501 (2010).
- [36] J. Twamley and S. D. Barrett, Superconducting cavity bus for single nitrogen-vacancy defect centers in diamond, *Phys. Rev. B* **81**, 241202 (2010).
- [37] Y. Matsuzaki and H. Nakano, Enhanced energy relaxation process of a quantum memory coupled to a superconducting qubit, *Phys. Rev. B* **86**, 184501 (2012).
- [38] S. Saito, X. Zhu, R. Amsüss, Y. Matsuzaki, K. Kakuyanagi, T. Shimo-Okada, N. Mizuochi, K. Nemoto, W. J. Munro, and K. Semba, Towards Realizing a Quantum Memory for a Superconducting Qubit: Storage and Retrieval of Quantum States, *Phys. Rev. Lett.* **111**, 107008 (2013).
- [39] B. Julsgaard, C. Grezes, P. Bertet, and K. Mølmer, Quantum Memory for Microwave Photons in an Inhomogeneously Broadened Spin Ensemble, *Phys. Rev. Lett.* **110**, 250503 (2013).
- [40] I. Diniz, S. Portolan, R. Ferreira, J. M. Gérard, P. Bertet, and A. Auffeves, Strongly coupling a cavity to inhomogeneous ensembles of emitters: Potential for long-lived solid-state quantum memories, *Phys. Rev. A* **84**, 063810 (2011).
- [41] X. Zhu, Y. Matsuzaki, R. Amsüss, K. Kakuyanagi, T. Shimo-Okada, N. Mizuochi, K. Nemoto, K. Semba, W. J. Munro, and S. Saito, Observation of dark states in a superconductor diamond quantum hybrid system, *Nat. Commun.* **5**, 3424 (2014).
- [42] N. Skribanowitz, I. P. Herman, J. C. MacGillivray, and M. S. Feld, Observation of Dicke Superradiance in Optically Pumped HF Gas, *Phys. Rev. Lett.* **30**, 309 (1973).
- [43] M. Gross, C. Fabre, P. Pillet, and S. Haroche, Observation of Near-infrared Dicke Superradiance on Cascading Transitions in Atomic Sodium, *Phys. Rev. Lett.* **36**, 1035 (1976).
- [44] J. M. Raimond, P. Goy, M. Gross, C. Fabre, and S. Haroche, Collective Absorption of Blackbody Radiation by Rydberg Atoms in a Cavity: An Experiment on Bose Statistics and Brownian Motion, *Phys. Rev. Lett.* **49**, 117 (1982).
- [45] M. Scheibner, T. Schmidt, L. Worschel, A. Forchel, G. Bacher, T. Passow, and D. Hommel, Superradiance of quantum dots, *Nat. Phys.* **3**, 106 (2007).
- [46] R. Röhlsberger, K. Schlage, B. Sahoo, S. Couet, and R. Rüffer, Collective Lamb shift in single-photon superradiance, *Science* **328**, 1248 (2010).
- [47] R. G. DeVoe and R. G. Brewer, Observation of Superradiant and Subradiant Spontaneous Emission of Two Trapped Ions, *Phys. Rev. Lett.* **76**, 2049 (1996).
- [48] J. Eschner, Ch. Raab, F. Schmidt-Kaler, and R. Blatt, Light interference from single atoms and their mirror images, *Nature (London)* **413**, 495 (2001).
- [49] S. Filipp, M. Göppel, J. M. Fink, M. Baur, R. Bianchetti, L. Steffen, and A. Wallraff, Multimode mediated qubit-qubit coupling and dark-state symmetries in circuit quantum electrodynamics, *Phys. Rev. A* **83**, 063827 (2011).
- [50] A. F. Van Loo, A. Fedorov, K. Lalumière, B. C. Sanders, A. Blais, and A. Wallraff, Photon-mediated interactions between distant artificial atoms, *Science* **342**, 1494 (2013).
- [51] J. A. Mlynek, A. A. Abdumalikov, C. Eichler, and A. Wallraff, Observation of Dicke superradiance for two artificial atoms in a cavity with high decay rate, *Nat. Commun.* **5**, 5186 (2014).

- [52] D. Meiser and M. J. Holland, Steady-state superradiance with alkaline-earth-metal atoms, *Phys. Rev. A* **81**, 033847 (2010).
- [53] J. Keaveney, A. Sargsyan, U. Krohn, I. G Hughes, D. Sarkisyan, and C. S. Adams, Cooperative Lamb Shift in an Atomic Vapor Layer of Nanometer Thickness, *Phys. Rev. Lett.* **108**, 173601 (2012).
- [54] S. J. Roof, K. J. Kemp, M. D. Havey, and I. M. Sokolov, Observation of Single-photon Superradiance and the Cooperative Lamb Shift in an Extended Sample of Cold Atoms, *Phys. Rev. Lett.* **117**, 073003 (2016).
- [55] T. P. Orlando, J. E. Mooij, L. Tian, C. H. van der Wal, L. S. Levitov, S. Lloyd, and J. J. Mazo, Superconducting persistent-current qubit, *Phys. Rev. B* **60**, 15398 (1999).
- [56] J. R. Johansson, P. D. Nation, and F. Nori, QuTiP: An open-source Python framework for the dynamics of open quantum systems, *Comput. Phys. Commun.* **183**, 1760 (2012).
- [57] J. R. Johansson, P. D. Nation, and F. Nori, QuTiP 2: A Python framework for the dynamics of open quantum systems, *Comput. Phys. Commun.* **184**, 1234 (2013).
- [58] V. V. Temnov and U. Woggon, Superradiance and Subradiance in an Inhomogeneously Broadened Ensemble of Two-Level Systems Coupled to a Low-Q Cavity, *Phys. Rev. Lett.* **95**, 243602 (2005).
- [59] M. Delanty, S. Rebic, and J. Twamley, Superradiance and phase multistability in circuit quantum electrodynamics, *New J. Phys.* **13**, 053032 (2011).
- [60] B. Bartels and F. Mintert, Smooth optimal control with Floquet theory, *Phys. Rev. A* **88**, 052315 (2013).
- [61] T. Nöbauer, A. Angerer, B. Bartels, M. Trupke, S. Rotter, J. Schmiedmayer, F. Mintert, and J. Majer, Smooth Optimal Quantum Control for Robust Solid-state Spin Magnetometry, *Phys. Rev. Lett.* **115**, 190801 (2015).
- [62] J. Zhang, Y.-x. Liu, R.-b. Wu, K. Jacobs, and F. Nori, Quantum feedback: Theory, experiments, and applications, *arXiv:1407.8536*.
- [63] F. Yoshihara, Y. Nakamura, F. Yan, S. Gustavsson, J. Bylander, W. D. Oliver, and J. S. Tsai, Flux qubit noise spectroscopy using Rabi oscillations under strong driving conditions, *Phys. Rev. B* **89**, 020503 (2014).
- [64] G. C. Knee, K. Kakuyanagi, M.-C. Yeh, Y. Matsuzaki, H. Toida, H. Yamaguchi, A. J. Leggett, and W. J. Munro, A strict experimental test of macroscopic realism in a superconducting flux qubit, *Nat. Commun.* **7**, 13253 (2016).
- [65] N. Lambert, K. Debnath, A. F. Kockum, G. C. Knee, W. J. Munro, and F. Nori, Leggett–Garg inequality violations with a large ensemble of qubits, *Phys. Rev. A* **94**, 012105 (2016).